# Modelling Pattern Recognition in Cricket Phonotaxis

by

Thomas Rost

A thesis submitted to Technische Universität Berlin

in partial fulfilment of the degree of

Master of Science

Bernstein Center for Computational Neuroscience

March 2011




supervisor: Prof. Martin P. Nawrot

## Declaration

Except where acknowledged in the customary manner, the material presented in this thesis is, to the best of my knowledge, original and has not been submitted in whole or part for a degree in any university.

Thomas Rost

_____

## Acknowledgements

Martin Nawrot, Farzad Farkhooi, Matthias Hennig, Jannis Hildebrandt, Chris Häusler, Laura Block

**Abstract**

A spiking neuron implementation of pattern recognition of the calling songs in *Gryllus bimaculatus* is proposed. A simplified model of the auditory interneuron AN1 has been fitted to extracellular physiological data. The model captures the aspects of AN1's rate-response to acoustic stimulation which are believed to be sufficient for pattern recognition. Stimulation patterns can be induced into the model via current injecton of the signals envelope-shapes. The model was used as the input stage to the pattern recognition mechanisms. A biologically plausible filter mechanism for pulse-pause patterns is proposed which is based on short term synaptic plasticity. Three simple filter mechanism are described, based on either isolated synaptic depression or synaptic facilitation. These filters are able to reproduce physiological findings from the cricket's auditory brain neurons. Further, it is argued that more complex filters can be produced by using combinations of depression and facilitation, and that a complete model of the cricket's pattern recognition apparatus may be implemented in this way. This however is left as a subject of further studies.

# Contents

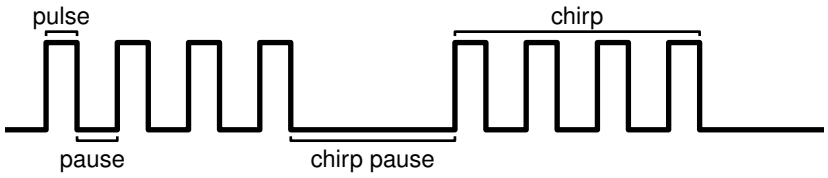


**Figure 1:** Schematic envelope of the cricket's calling song (adapted from [Hennig, 2009]).

# 1 Introduction

## 1.1 Phonotaxis

Crickets, like various other insects, use acoustic communication for their sexual selection [Pollack, 2000]. Male specimen rub their wings together, producing sounds which attract females. The behavioural aspects of cricket phonotaxis have widely been studied (e.g. [Hedwig & Poulet, 2005], [Hedwig, 2006], [Hennig, 2009], [Nabatiyan et al., 2003], [Schildberger, 1984]). Females use the sound for localization, as well as to assess the attractiveness of their mating partners [Hedwig, 2006]. The songs consist of packages of pulses of near pure tones with frequencies around 4.5 kHz which are referred to as *chirps*. Pauses between the chirps produce the characteristic cricket songs. A schematic envelope of such a song is shown in figure 1. The signal can be parametrized by the pulse duration, pause duration, number of pulses per chirp and the length of the pauses between chirps. In [Hennig, 2009], experiments are described in which crickets were presented with artificially generated sound patterns. The animals were placed on locomotion-compensators, so that their movements could be recorded. It was shown that varying the song parameters influences the animals inclination to approach a sound source. For certain configurations of song patterns, the crickets show strong positive phonotaxis while others leave them unimpressed (for similar results see [Hedwig & Poulet, 2005], [Schildberger, 1984]). This is illustrated in figure 2, which shows the phonotactic efficiency of patterns with various pulse and pause durations. The mechanisms by which crickets recognize and assess patterns are not fully understood. It is however widely assumed that some kind of *filter* is implemented in their brain.

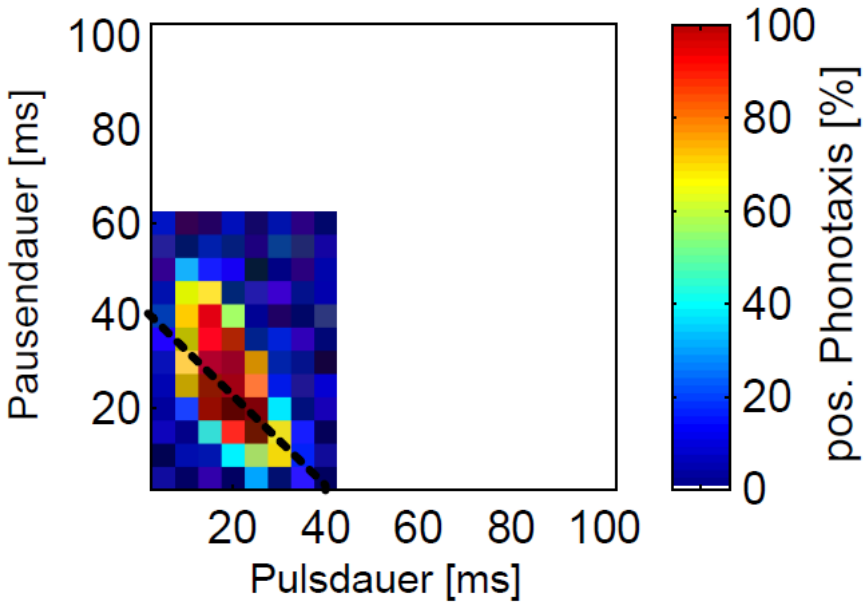


**Figure 2:** Behavioural response of female crickets to calling songs with various pulse and pause durations. The percentage phonotaxis was calculated as the ratio of specimen which showed positive phonotaxis in response to each pattern. (figure taken from [Hildebrandt, esis])

## 1.2 Neurophysiology

Crickets represent an attractive model-organism because of the relatively small size of their nervous system. An overview of the auditory system of *Gryllus bimaculatus* relevant for phonotaxis will be given in the following.

From the cricket's ears, which reside in the front legs, about 60 auditory receptors project into the prothoracic ganglion [Hedwig, 2006]. Here, three types of auditory interneurons have been identified. The Ascending Neuron 1 (AN1) responds mainly to stimulation with frequencies around 4.5 kHz, the frequency of the cricket's calling song [Wohlers & Huber, 1978]. The Ascending Neuron 2 (AN2) responds mainly to ultrasonic frequencies [Schildberger, 1984] used for echolocation by insectivorous bats [Faulkes & Pollack, 2000]. The third type of interneuron is the Omega Neuron (ON). The ONs also receive auditory receptor input. All three types of interneurons exist for both sides of the cricket. The ON-cells inhibit the contralateral interneurons [Hedwig, 2006], while the ANs project into the brain [Schildberger, 1984]. All interneurons copy the pulse structure of calling songs and seem to perform no significant filtering or pattern discrimination [Nabatiyan et al., 2003].

In the cricket brain, Schildberger has identified two main types of neurons responding to auditory stimulation: BNC1, which have arborizations overlapping with those of the ascending cells, and BNC2, which receive no input from the ascending cells [Schildberger, 1984]. These brain neurons exhibit characteristic filter properties which are very likely involved in pattern recognition. The filter properties of the brain neurons as measured by Schildberger are shown in figure 3.

## 1.3 Proposed filter mechanisms

It is widely assumed that the filtering of attractive patterns takes place in the brain. Two types of mechanisms that could achieve such an effect have been proposed:

1. Hoy [Hoy, 1974] states that the motor-patterns producing the calling songs are generated in the central brain and hypothesises that recognition of attractive patterns could be achieved by comparison of an external pattern to the internal *template*. Hennig [Hennig, 2003] has proposed that cross-correlation between an internal template and the external pattern may be implemented in the cricket brain. This mechanism is able to reproduce the dependence of phonotactic behaviour on the temporal structure of the calling song. However, no physiological evidence of an internal template generator has so far been found in the cricket brain.

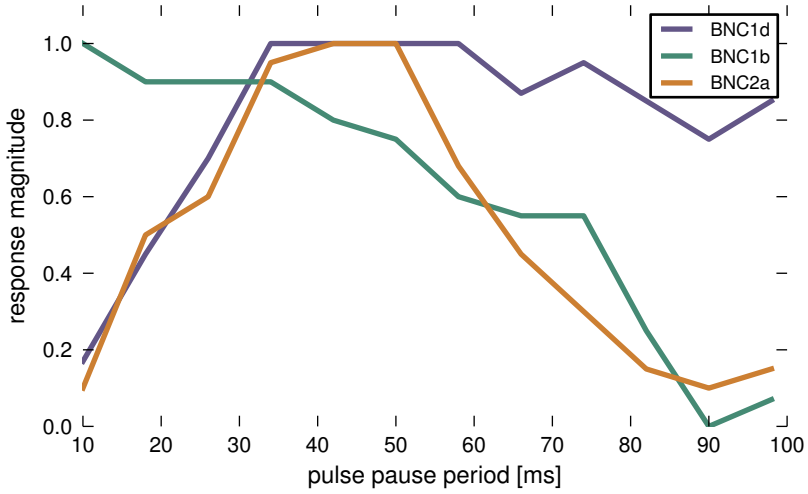


**Figure 3:** Reproduction of the pulse-pause filters measured by Schildberger (Values measured from figure 12 in [Schildberger, 1984]). Pulse pause patterns with constant duty cycle and varying period were presented to the crickets. The response curve was then generated by normalising the spike count over a 250 ms window. Low-pass (BNC1d), high-pass (BNC1b) and band-pass filters (BNC2a) are shown.

2. Schildberger [Schildberger, 1984] has described the filter properties of the BNC cells (see figure 3). He proposed that low and high-pass filters with respect to pulse duration exist, and that the summation of their outputs can lead to band-pass properties. Since Schildberger kept the duty cycle of his stimulation-patterns constant, it is not possible to distinguish between pulse and pause filters. However, this is the only physiologically backed filter mechanism proposed so far.

## 1.4 Aims of this study

The aim of this study was to produce a neuronal model of pattern recognition in cricket phonotaxis. Webb et al. [Webb & Scutt, 1997] have produced a spiking neuron model of the cricket's auditory system which can successfully control a robot which mimics phonotactic behaviour. They have however mainly concentrated on the directional processing of information.

Here on the other hand, it was attempted to propose a model for the recognition of attractive calling song patterns. Wittmann [Wittmann et al., 2010] has

presented a pattern recognition model for the locust, based on an artificial neural network, that performs with some success. The fact that parameters of the songs are fed into the network as abstract features however, ignores the step of actually extracting these features from the songs and bears no biological relevance.

The aim was here, to produce a model which takes as its input the envelope of a calling song, and produces an output that can be related to behavioural results for a particular type of pattern. Since the only physiological evidence about filtering mechanisms in the cricket brain is that of Schildberger [Schildberger, 1984], his work was used as a guideline.

To produce an input to the filter-neurons in the brain, parts of the auditory system had to be modelled as well. Since sound localization was ignored in this study, and auditory information from both sides is kept separate in the brain [Hedwig, 2006], only one half of the system was modelled. Further, because the ONs seem to be involved in directional processing and the AN2s are mainly important for predator avoidance (see section 1.2), only the AN1 and BNC cells were considered.

The generation of an AN1 model based on extracellular recordings and some ideas for BNC-filter implementations are described in the following sections.

# 2 Data analysis

The data used here was generated by Jannis Hildebrandt in the lab of Matthias Hennig at the Institute for Theoretical Biology, Humboldt University Berlin for his Diploma thesis [Hildebrandt, esis] and was kindly provided for the purpose of this study.

## 2.1 Nature of the data

Extracellular recordings of AN1 were performed on 13 individual crickets (*Gryllus bimaculatus*). All specimen were grown up females, obtained from a commercial supplier. All recordings were made using hook electrodes placed at the axons ascending from the auditory interneurons to the brain. The recordings were digitized at a sample rate of 20 kHz. Spikes were then detected using a threshold technique, and sorted according to their amplitude. The action potentials of AN1 have a lower amplitude than those produced by AN2.

Two stimulation paradigms were carried out. The first one was aimed at determining the intensity response curve of the cells. For this purpose, contin-

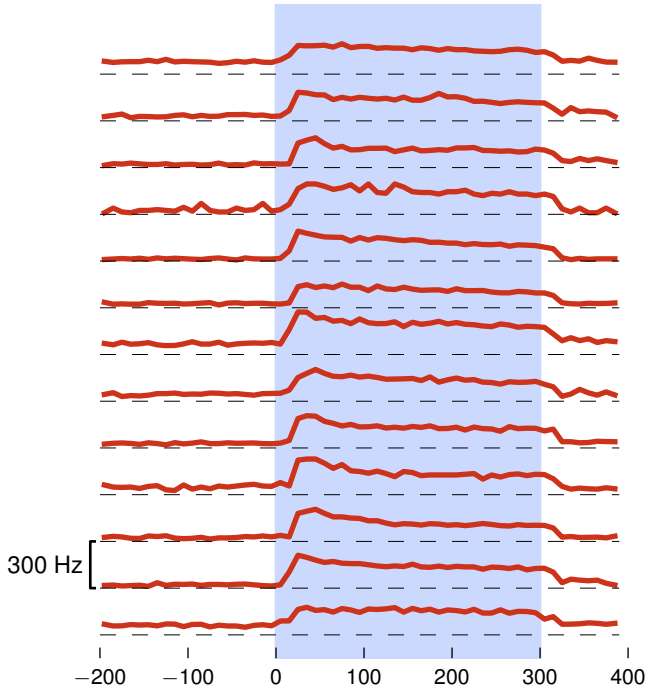


**Figure 4:** Spike rate estimates for all 13 AN1s in the data for the 300 ms stimulations used to determine the intensity response curves. Only trials with intensities of 78 and 84 dB were taken into account.

| $f_{spont}[Hz]$ | $f_0[Hz]$ | $f_\infty[Hz]$ | $\tau_{eff}[ms]$ (c) | $\tau_{eff}[ms]$ (uc) |
|---|---|---|---|---|
| 21.5 | 209.2 | 131.3 | 42.9 | **66.6** |
| 25.5 | 202.7 | 105.6 | 61.9 | 63.8 |
| 52.0 | 241.3 | 124.4 | 45.7 | 43.8 |
| 34.2 | 189.1 | **127.0** | 67.4 | 31492.1 |
| 30.7 | 222.0 | 124.9 | 33.7 | 30.6 |
| 47.1 | 186.7 | 127. | 75.3 | 109.7 |
| 71.8 | 278.4 | 188.2 | 43.5 | 42.4 |
| 27.9 | 153.3 | 105.6 | 80.6 | 51682.1 |
| 13.8 | **194.8** | 106.5 | 78.0 | 242.5 |
| **33.0** | 212.0 | 135.6 | **66.1** | 236.4 |
| 21.5 | 194.5 | 112.3 | 28.8 | 27.2 |
| 59.5 | 180.2 | 149.6 | 68.2 | 21.3 |
| 77.4 | 192.1 | 152.4 | 93.5 | 278.8 |

**Table 1:** Summary of characteristics extracted from the data shown in figure 4. Bold values indicate medians. The two values for the adaptive time constant $\tau_{eff}$ are for the constrained (c) and unconstrained (uc) estimation methods (see section 2.2)

uous sounds of 300 ms length were presented to the specimen at intensities ranging from 30 to 84 dB. Rate estimates from these stimulations for all 13 AN1 cells are shown in figure 4. Since the following stimuli were presented at an intensity of 80 dB, only trials with stimulus intensities of 78 and 84 dB were used to estimate the rates. This data was used to characterise the response of the neurons. Table 1 shows the peak and steady state rates for all neurons.

For the second paradigm, pulse-pause-patterns with different parameters were presented to the animals. Here pulse durations and pause lengths were varied independently between 5 and 100 ms in increments of 5 ms. These patterns were presented at an intensity of 80 dB. Each stimulus started with a 200 ms pulse, intended to bring the interneurons to a defined adaptation state. This pulse was always followed by a 20 ms pause. Pulses and pauses were then repeated, ending with a pause, until the total duration was just under 800 ms. The stimulus was then ended with a 200 ms block, to compare the adaptation states at beginning and end of each stimulation. Hence stimuli had varying lengths of up to 1 s. The stimuli can be seen as shaded areas in figure 5. Each stimulus was presented to each animal in blocks of 10 to 12 repetitions.

Figure 5 also shows spike trains and Peri Stimulus Time Histograms (PSTHs) for four different neurons from the data set. The top panel shows a high frequency pattern, in which both pulse and pause are short (10 ms). The changes are too fast for the neuron, and no significant synchrony between the stimulus

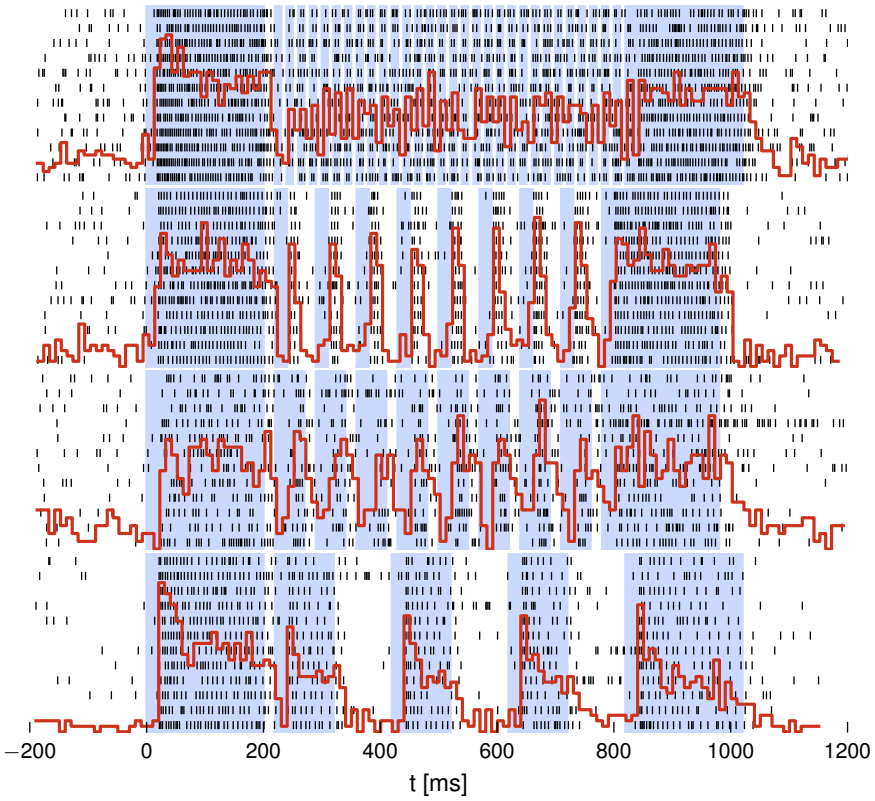


**Figure 5:** Sample AN1 spike trains from the data for different neurons and conditions. Shaded areas indicate stimulation patterns for four different combinations of pulse and pause duration. Superimposed PSTHs have arbitrary scaling.

and firing rate is evident. In the second panel, the pulse duration is 20 ms and the pause duration is 50 ms. It can be seen that the spike rate follows the stimulation pattern with a delay of about 20 ms. In the bottom panel, both pulse and pause lengths were 100 ms. The longer pulses reveal that the neurons also show spike-frequency adaptation i.e. the relaxation of an initially high rate to a lower level in response to a continuous input, within the pulse presentations.

Since all the pulse pause patterns were presented at a single intensity level, the response of the neurons can be adequately characterized by their spontaneous rate ($f_{spont}$), the peak rate after stimulus onset ($f_0$), the equilibrium rate ($f_\infty$) and the time constant of adaptation ($\tau_{eff}$). The extraction of the rates from the data is trivial. The estimation of $\tau_{eff}$ will be explained in the following.

## 2.2 Estimating the time-constant of adaptation

Benda et al. estimated the effective time constant of adaptation for auditory inter neurons in the *locust*. The procedure described in [Benda & Hennig, 2008], has been adopted here. They assumed an exponential function of the form:

$$f(t) = (f_0 - f_\infty) \exp\left(-\frac{t}{\tau_{eff}}\right) + f_0 \tag{1}$$

This equation was fitted to the spike rate using a least squares method. The rate was estimated for each millisecond as the trial averaged inverse of all inter-spike intervals containing that bin. The resultant time course of the spike frequency was then smoothed using a 3 ms rectangular sliding window. In [Benda & Hennig, 2008], the values for $f_0$ and $f_\infty$ were simply taken as the first peak after stimulus onset and the average rate in a short window before the end of the stimulus. These values however can also be fitted by the least squares method. Both methods (constrained and unconstrained) were tested here. Figure 6 shows the spike rate estimates and fitted exponentials for three different neurons. In the top panel, the spike rate closely resembles an exponential shape. In this case, the difference between the constrained and unconstrained estimates for $\tau_{eff}$ differ only minimally. If the shape of the of the response is less similar to the exponential function, the two estimates diverge. The constrained estimate seems to give more stable, but not necessarily more realistic results. Looking at table 1 however, it can be seen that the medians across all neurons differ only marginally for the two estimation methods.

Looking at figures 4 and 5, it can be seen that the recordings show a significant firing rate before stimulus onset (median: 29 Hz). Boyan et al. [Boyan & Williams, 1982] reported that AN1 neurons have spontaneous rates of 30 to 40 Hz. They found however that this activity is suppressed during

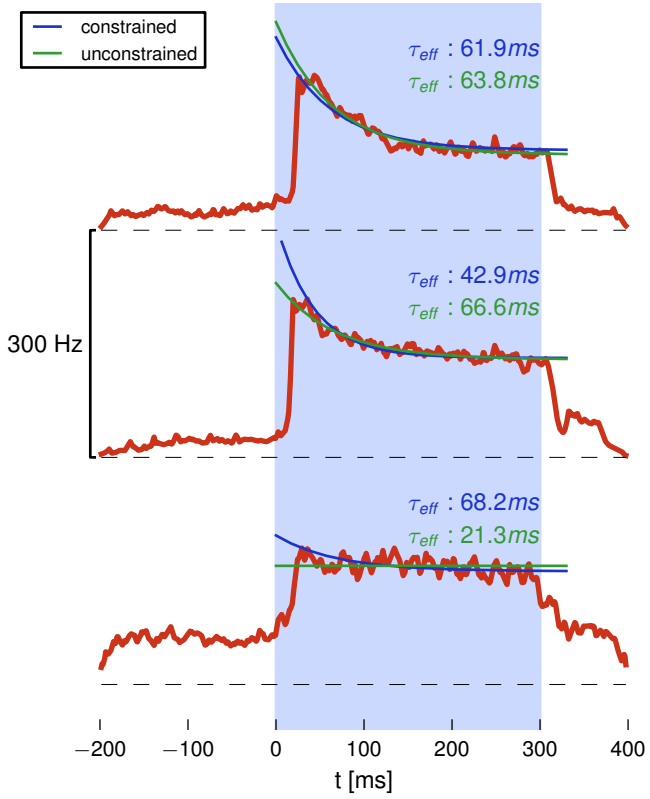


**Figure 6:** Illustration of the estimation of the effective adaptive time constant for three of the neurons. In the constrained case $\tau_{eff}$ was the only free parameter of the exponential function. In the unconstrained case, the peak- and steady state rates were also fitted using least squares method.

| $f_{spont}[Hz]$ | $f_0[Hz]$ | $f_\infty[Hz]$ | $\tau_{eff}[ms]$ |
|---|---|---|---|
| 0. | 165. | 91. | **66.6** |

**Table 2:** Characteristics of a *standard AN1*, corrected for background activity in the extracellular spike data.

auditory stimulation and that it vanishes completely during long stimulations. Schildberger [Schildberger, 1988] reports that AN1 shows no or little spontaneous activity. It was therefore be concluded, that the extracellular recordings contain spikes from other cells which were not excluded during spike sorting. However, since the rate-response of AN1 is very strong, it can be assumed that the rates are dominated by that cell. To obtain an estimate of the isolated activity of AN1, which is fed in to the brain neurons, the baseline activity was simply subtracted from the rates. Taking the difference of medians, this lead to the *standard AN1* which is characterised by the values in table 2.

# 3 Modelling AN1

## 3.1 Neuron model

All simulations were carried out using the BRIAN-simulator [1]. The neuron model used for this study was a simple leaky integrate and fire neuron (adapted from [Muller et al., 2007]) :

$$C_m \frac{dV_m}{dt} = \sum_i g_i \left(E_i - V_m\right) + I_{ext} \tag{2}$$

Here, $C_m$ is the membrane capacitance, $V_m$ is the membrane potential, $g_i$ and $E_i$ are the conductances and reversal potentials of the various membrane currents and $I_{ext}$ is an additional external current. The following currents were modelled:

- leak current:

$$\begin{aligned} & g_l(E_l - V_m) \\ & g_l = constant \end{aligned} \tag{3}$$

[1] www.briansimulator.org

- excitatory synaptic input:

$$g_e(E_e - V_m) \tag{4}$$
$$\frac{dg_e}{dt} = -\frac{g_e}{\tau_e} + q_e\delta(t - t_s)$$

  $q_e$ is the quantal conductance increase for spikes arriving at excitatory synapses at times $t_s$.

- spike-frequency adaptation:

$$g_{sfa}(E_{sfa} - V_m) \tag{5}$$
$$\frac{dg_{sfa}}{dt} = -\frac{g_{sfa}}{\tau_{sfa}} + q_{sfa}\delta(t - t_s)$$

  here $t_s$ are the times when the unit itself spikes.

- the external current $I_{ext}$. For ease of implementation this was split up into three components.

$$I_{ext} = I_s + I_{in} + I_{noise} \tag{6}$$

  Here $I_s$ is a constant current which produces the spontaneous rate of the unit. $I_{in}$ is used to inject stimulus patterns, and $I_{noise}$ is modelled as an Ornstein-Uhlenbeck process, which produces exponentially correlated noise. It has the form (from [Fox et al., 1988]):

$$\frac{dI_{noise}}{dt} = -\frac{I_{noise}}{\tau_{noise}} + G_w \tag{7}$$

  $G_w$ is a random variable from a Gaussian distribution which is added to the derivative in each time step. This noise process is meant to mimic the synaptic filtering of background activity received by the neuron.

Figure 7 illustrates how the model-currents converge to an equilibrium state after a simulation is started with a constant current injection. After about 300 ms the spike rate assumes a steady state value.

Figure 8 shows the different behaviours of the spike rate in response to a step input that can be achieved by varying the parameters of the adaptive current (equation 6) $\tau_{sfa}$ and $q_{sfa}$. Although AN1 is assumed to have no spontaneous activity, a small amount of current ($I_s$) was constantly injected into the units, producing a spontaneous rate of about 1 Hz. Combined with a *warm-up time* of 300 ms before each run, this was aimed at allowing the model currents to reach a defined equilibrium state before the onset of stimulation.

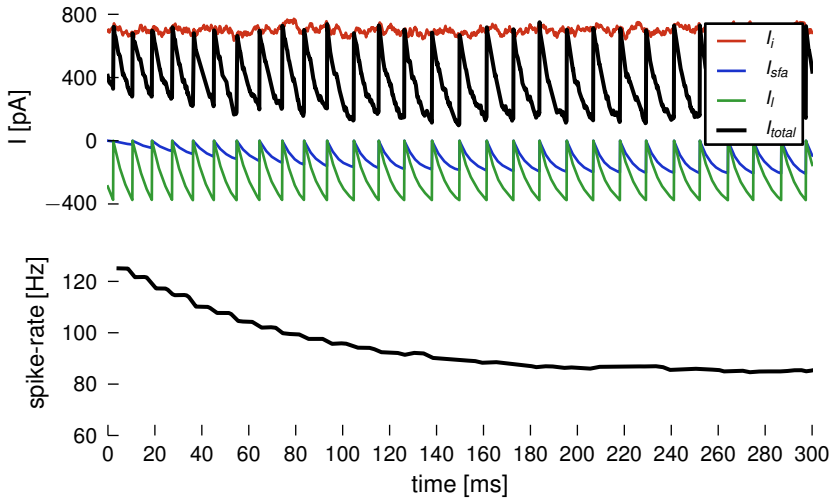


**Figure 7:** Illustration of the membrane-currents of the model in response to a constant current injection. After some time, the input current $I_i$ is balanced by the adaptation-current $I_{sfa}$ and the membrane leakage $I_l$ and the spike rate assumes a steady-state value. The rate shown in the lower panel was estimated for a population of 100 units with the same parameters as the one shown in the upper panel.

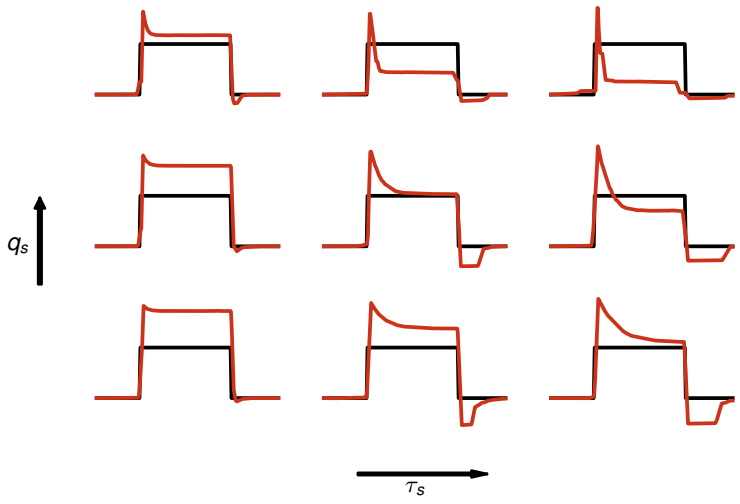


**Figure 8:** Spike-rate of the model in response to a step current-input, showing the different behaviours dependant on $q_{sfa}$ and $\tau_{sfa}$.

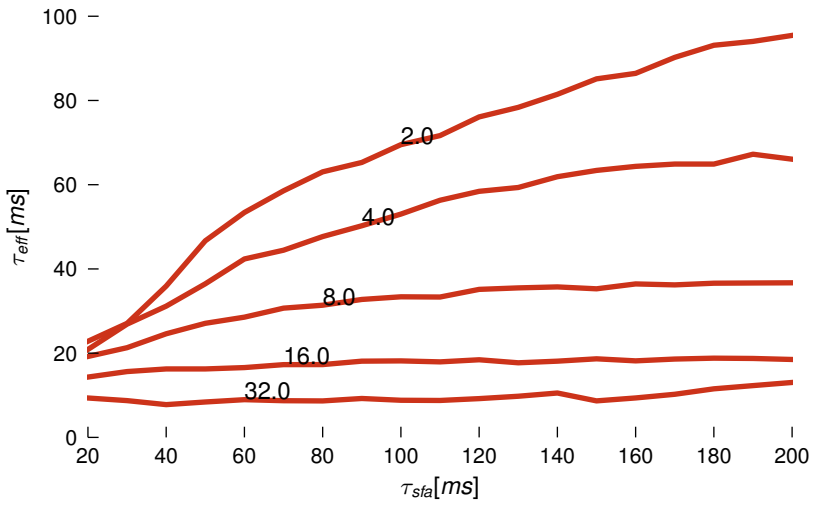


**Figure 9:** Effective adaptive time constant $\tau_{eff}$ of the model versus the time constant of the the adaptive current $\tau_{sfa}$. The numbers on the graph indicate the values of the increment parameter $q_{sfa}$ in $nS$.

## 3.2 Parameter fitting

No biologically realistic parameters for the Integrate and Fire model of AN1 (e.g. membrane time constant and impedance) could be found in the literature. Therefore the basic parameters given in [Muller et al., 2007] were used if not otherwise stated.

For the purpose of this study, i.e. providing an input to the pattern recognition mechanism, the response of the AN1 neuron is sufficiently characterized by the rate levels in response to a stimulus of 80 dB intensity and its time constant of adaptation. In section 2 it was shown, that the rate responses of the 13 neurons inspected varied considerably. It was therefore decided to fit the model to the median values indicated in table 2.

The stimulus patterns were presented to the model neurons as direct current injections. The adaptation behaviour was adjusted by tuning the parameters $\tau_{sfa}$ and $q_{sfa}$.

Figure 9 shows the effective adaptation time constant $\tau_{eff}$ plotted versus the model time constant $\tau_{sfa}$ for various values of the incremental parameter $q_{sfa}$. Since changing the adaptation parameters also changes the rate response to a given level of input current, the input currents for spontaneous activity and pattern input had to be tuned for each point in the plot individually to achieve

| parameter | value | |
|---|---|---|
| $C_m$ | 289.5 pF | membrane capacitance |
| $g_l$ | 28.95 nS | leak conductance |
| $V_{reset}$ | -70 mV | reset voltage |
| $V_{threshold}$ | -57 mV | spike threshold |
| $E_l$ | -70 mV | leak reversal potential |
| $E_e$ | 0 mV | synaptic reversal potential |
| $\tau_e$ | 1.5 ms | synaptic time constant |
| $E_{sfa}$ | -70 mV | sfa-current reversal potential |
| $\tau_{sfa}$ | 120 ms | time constant of sfa-current |
| $q_{sfa}$ | 3. nS | incremental parameter of sfa-current |
| $I_s$ | 390. pA | current producing the spontaneous rate |
| $I_{in}$ | 470. pA | stimulation current level |
| $\tau_{noise}$ | 1.5 ms | time constant of the noise process |
| $\sigma_{noise}$ | 39. pA | standard deviation of the added noise |

**Table 3:** summary of parameters of the final AN1 model.

the desired values for $f_{spont}$, $f_0$ and $f_\infty$. The necessary current levels were determined by using the bisection method, and the currents were only tuned to a certain accuracy. This explains the lack of smoothness in the curves for a given value of $q_{sfa}$. From the data shown in the figure, the pair of $\tau_{sfa}$ and $q_{sfa}$ were taken which gave the value of $\tau_{eff}$ closest to the median of the values extracted from the data. The parameters were then fine-tuned manually to achieve the desired result.

To mimic the intrinsic variability present in all neurons, a small amount of noise was added to the model. The Gaussian noise $G_w$ (see equation 7) was scaled to have a standard deviation of 10 % of the amplitude of the spontaneous current $I_s$. The time constant of the noise process $\tau_{noise}$ was set to 1.5 ms, resembling synaptic filtering.

All parameters used in the final model are summarized in table 3.

### 3.3 Results

Figure 10 shows the response of the final AN1 model to a step input. The top panel shows sample spike trains. In the bottom panel, a rate estimate is shown with the fitted exponential function superimposed. It can be seen that the model produces the correct effective time constant of adaptation and approximately the right peak and steady state rates. The spike trains look very regular. This is in accordance with the intracellular recordings shown in

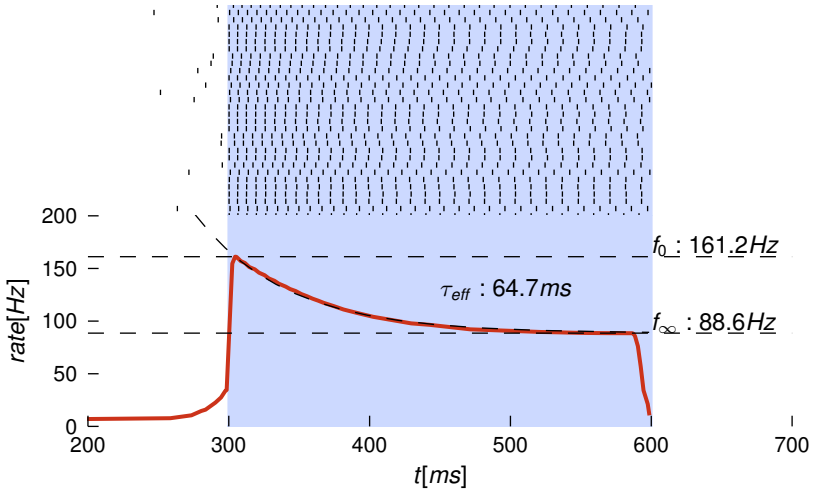


**Figure 10:** The upper panel shows sample spike trains of the fitted AN1 model in response to a step current-input. The lower panel shows a rate estimate over 100 trials with the resultant exponential fit and effective time constant superimposed. The decrease in rate before the end of the stimulus (marked by the blue shading) is an artefact of the rate estimation method.

[Boyan & Williams, 1982]. After the stimulus, the model is still in an adapted state and produces no spikes. This also matches the observations reported by Boyan [Boyan & Williams, 1982] that no spontaneous activity occurs during stimulation.

In figure 11, the spike rate of the model is compared to the physiological data. The median spontaneous rate of 29 Hz as well as the response latency of 20 ms were manually added to the spike frequency estimate to enable a comparison. The non-zero spike rates between pulses is an artefact of the rate estimation method (see section 2.2). Each panel displays the rates for a different stimulus patterns and from a different neuron. First of all it can be observed, that the extracellular rates are much noisier than the model response. This is partly the reason for the discrepancy in the spike rates. The model does however reproduce the main characteristics of the AN1 response. The adaptation behaviour in the initial 200 ms blocks is very similar. Also the adaptation across pulses is captured. In the top and bottom panels, the onset rates for each pulse follow the trend contained in the data. The neuron shown in the middle panel is an outlier in terms of adaptation behaviour. It seems to adapt much stronger within pulses than the model. This also becomes strongly evident in the final 200 ms block. The model was however fitted to a median based *standard AN1*

and can therefore not reproduce all aspects of the individual cells.

# 4 Modelling BNC

Kazama et al. [Kazama & Wilson, 2008] have reported short term depression in synapses in the drosophila olfactory system. One of the properties they associated with the effect is a tendency of the post-synaptic cells to respond only to stimulus onsets (see also [Nawrot et al., 2010]). This effect is also prominent in the intracellular recordings of cricket BNC neurons reported by Schildberger et al. [Schildberger, 1984]. Further, the fact that Kazama et al. found a large number of synapses between the units in question is also consistent with the large dendritic trees of the BNC neurons reported by Schildberger. Tripp et al. [Tripp & Eliasmith, 2010] have described the filtering properties of dynamic synapses. The above observations lead to the idea to investigate the filtering properties of dynamic synapses when applied to pulse pause patterns as they occur in cricket songs.

## 4.1 Short Term Plasticity model

Tsodyks and Markram have developed a phenomenological model of short term synaptic plasticity [Tsodyks et al., 1998]. The model handles depression as well as facilitation and is implemented in the BRIAN-simulator. It will be explained in the following [2]. Synaptic weights ($q_e$, see equation 4) are modulated by the quantity $ux \in [0, 1]$. $u$ and $x$ are referred to as resources in the model framework and are modelled as separate differential equations:

$$\frac{dx}{dt} = (1 - x) / \tau_d \tag{8}$$

$$\frac{du}{dt} = (U - u) / \tau_f \tag{9}$$

$\tau_d$ and $\tau_f$ are the time constants for synaptic depression and facilitation and $U \in [0, 1]$ is a parameter governing the ratio of the original weight that is modulated. Each pre-synaptic spike produces an update of the model variables:

$$x \to x\,(1 - u) \tag{10}$$

$$u \to u + U\,(1 - u) \tag{11}$$

[2] explanation taken from www.briansimulator.org/docs/stp.html

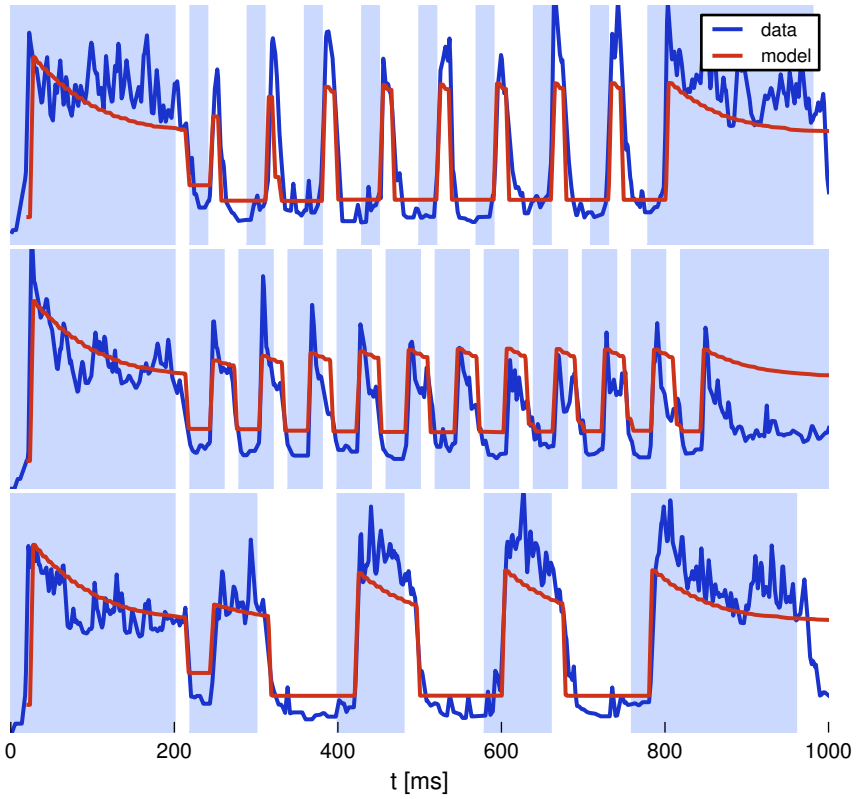


**Figure 11:** Comparison of model rates to rates estimated from the data for three different stimulation patterns. The physiological rates are from a different neuron in each panel. A delay of 20*ms* has been added manually to the model rates.

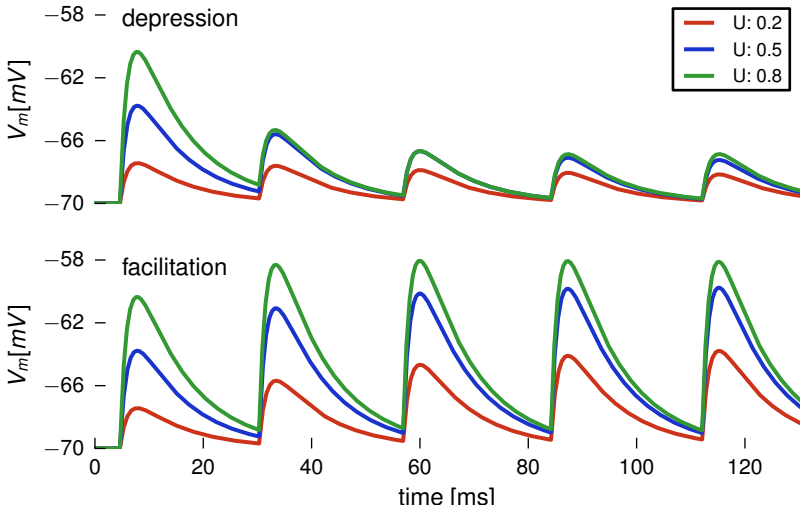


**Figure 12:** Illustration of the effect of the STP model on the post-synaptic membrane potential. The upper panel shows depression ($\tau_d$ = 100$ms$) for different values of the parameter $U$. The lower plot shows synaptic facilitation ($\tau_f$ = 100$ms$).

The effects of the parameters on the synaptic conductances are illustrated in figure 12. It can be seen that the parameter $U$ controls the magnitude of synaptic strength that is initially available. High values of $U$ combined with values of $\tau_d > \tau_f$ therefore lead to strong synaptic depression. Small values of $U$ and $\tau_f > \tau_d$ consequently produce facilitation. Combinations between those two extremes produce effects which are less intuitive.

## 4.2 Filter construction

It was here attempted to construct filters for the pulse pause patterns in the sense as described by Schildberger [Schildberger, 1984]. He presented the animals with artificial stimuli of 250 ms length, while the pulse and pause durations were varied from 4 to 49 ms. In each pattern, pulse and pause durations were equal. The filter curves were then constructed by plotting the normalised spike counts of individual brain-neurons in response to those stimuli over the pulse-pause period. Schildberger found *low-pass* and *high-pass* like filters for BNC1 cells and BNC2 cells showing *band-pass* - like filter properties. In the following, three types of filter which can be constructed using short-term synaptic plasticity will be explained.

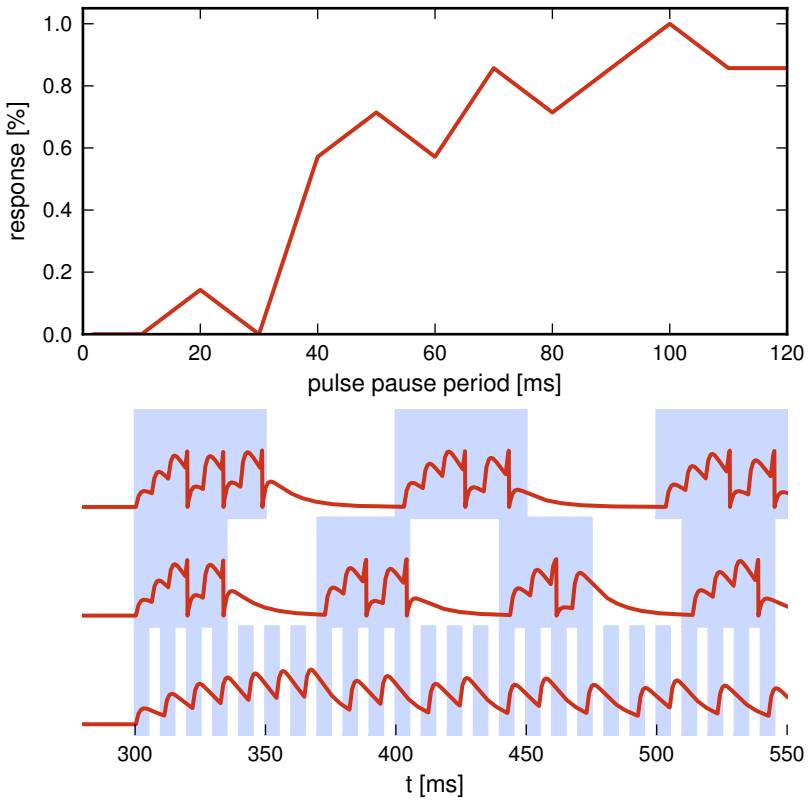


**Figure 13:** Illustration of a low-pass filter constructed using short-term facilitation. The upper panel shows the response curve as defined by Schildberger [Schildberger, 1984]. The lower panel shows the membrane potential of the filter neuron for several pulse/pause durations. The filter can be seen as a pulse-duration filter. If the pulse duration is sufficiently long, the facilitation causes the synaptic strength to increase and the unit fires. For shorter pulses, not enough synaptic weight is built up to cause the neuron to spike. (parameters: $w_{in} = 70nS$, $\tau_d = 0.01ms$,$\tau_f = 40ms$, $U = 0.2$ )

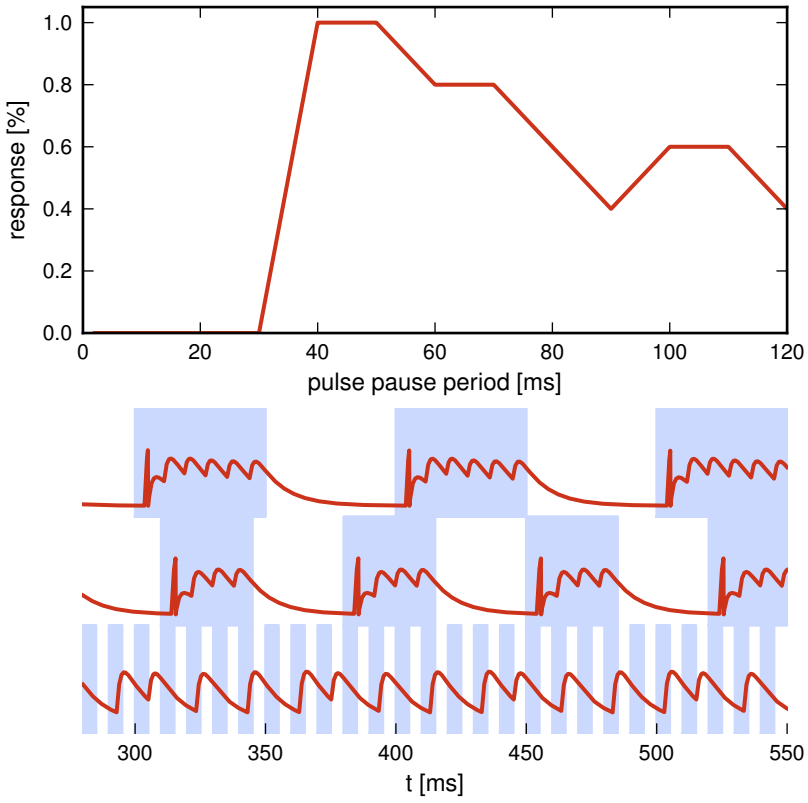


**Figure 14:** Illustration of a low-pass filter constructed using short-term depression. The unit acts as a pause filter. If the pauses are sufficiently long, the short term depression relaxes sufficiently to elicit a spike at the onset of the next pulse. (parameters: $w_{in} = 100nS$, $\tau_d = 30ms$,$\tau_f = 0.01ms$, $U = 0.8$ )

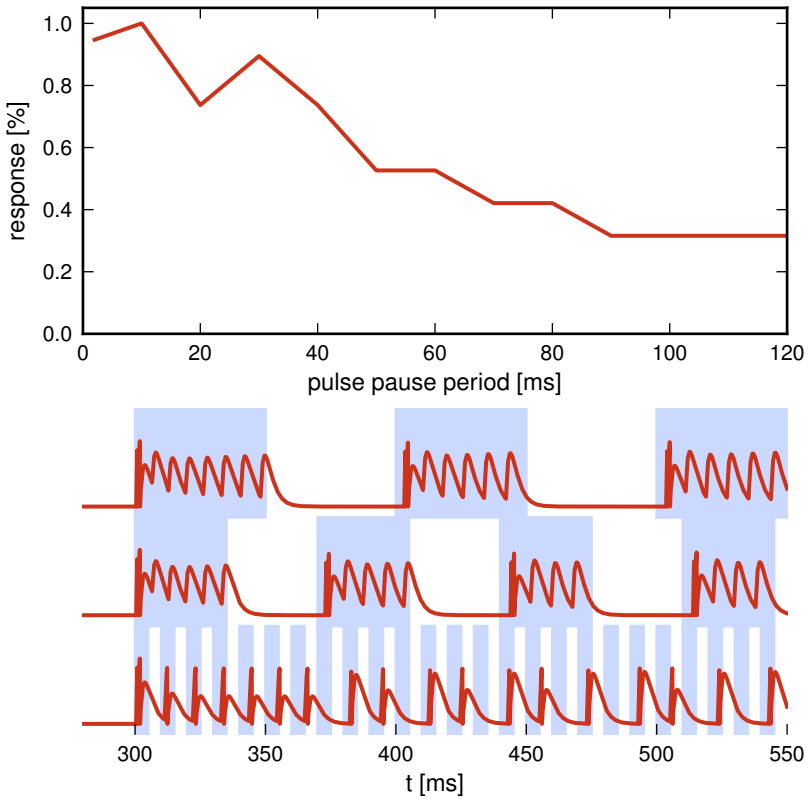


**Figure 15:** Illustration of a high-pass filter constructed using strong short-term depression. It acts effectively as a pulse onset detector. Since in the set-up described by Schildberger [Schildberger, 1984] the number of pulses per trial varies with pulse/pause frequency, this has the effect of a high pass filter. To achieve pulse onset detection for fast patterns, the membrane capacity had to be reduced by a factor 4. (parameters: $w_{in} = 45nS$, $\tau_d = 15ms$,$\tau_f = 0.01ms$, $U = 0.95$ )

Figure 13 shows a low pass filter, constructed using short term facilitation. The top panel shows the filter curve in the Schildberger sense. The model produces no spikes for very fast patterns and the rate then increases for patterns with longer periods. The jagged shape of the response curve is due to the varying number of pulses contained in the 250 ms counting interval which results from varying the pulse-pause period. The lower plot illustrates the way the filter operates for three different pulse-pause patterns. The post synaptic potential in the upper panel rises continually within each pulse, until several spikes are produced, giving high output counts for slow patterns. The middle plot shows an intermediate pulse length. Here, the facilitation is just strong enough to produce one or two spikes per pulse. The bottom trace shows that for very short pulses, facilitation is not strong enough to produce any spikes. The peaks of the post-synaptic potentials rise to a certain steady state level which stays below the threshold. This filter acts as a low-pass filter for pulse durations.

Another low-pass like filter can be constructed using short-term depression. This is shown in figure 14. Here, strong synaptic depression has been implemented. This has the effect, that a spikes are elicited only at the onset of pulses. During the pulses, the depressed synaptic weights fail to bring the membrane potential across the threshold. During the pauses, the depression relaxes again. If the pauses are sufficiently long, the synapses retain their original strength and cause the unit to fire again at the next pulse onset (see top two panels in figure 14). If the pauses become shorter, depression is still present at the onset of the next pulse and the unit fails to produce a spike. This means that the filter acts effectively as a pulse counter with a cut-off frequency depending on the pause length. The fall-off of the filter curve in the upper plot of figure 14 can be attributed to decreasing number of pulses in a pattern as the period is increased.

The third filter type that can be constructed is closely related to the previous one. It is also based on short-term depression and its behaviour is illustrated in figure 15. If the time constant of depression of the filter shown in figure 14 is reduced below the shortest pause length, the cut-off frequency vanishes and the unit becomes a pure pulse counter. To enable the unit to follow the faster pulse patterns, the membrane time constant had to be reduced by reducing the membrane capacitance $C_m$ by a factor 4. It must be assumed, that this filter only functions correctly in the Schildberger-set-up, where the number of pulses in the counting window varies with pattern-period.

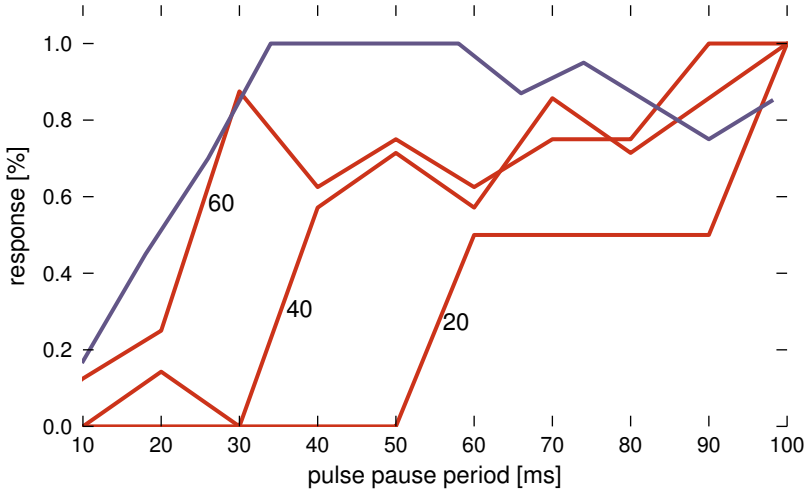


**Figure 16:** Response curves of low-pass filters using synaptic facilitation. The numbers in the plot indicate the values for $\tau_f$ in ms. All other parameters are as in figure 13. The purple line represents the low-pass filter extracted from Schildberger [Schildberger, 1984] (cf. figure 3).

## 4.3 Results

The response curves of the filters described in the previous section depend on the choice of time constant used for the short-term plasticity model. for each filter, the response has been calculated using different time constants. This is illustrated in figures 16 through 18. In figure 16 it can be seen that increasing the time constant of facilitation for the low pass filter shifts the cut off frequency towards faster patterns. This is intuitive, because the facilitation filter depends on a decay of synaptic strength during the pauses. If the time constant of facilitation is increased, a higher level of facilitation is maintained across pauses for fast patterns, enabling the unit to fire also during short pulses. The superimposed Schildberger-line shows that cut-off frequencies similar to the physiological results can be achieved using this type of filter.

Since the low-pass filter based on depression is an onset-detector which cuts off at low pattern periods because the depression is carried over the pauses, the dependence on the time constant has the opposite sense as for facilitation (see figure 17). As $\tau_d$ decreases, the minimum pause duration over which depression can be maintained decreases and the cut-off frequency of the filter increases.

If $\tau_d$ is reduced even further, the cut-off vanishes, and the filter becomes the

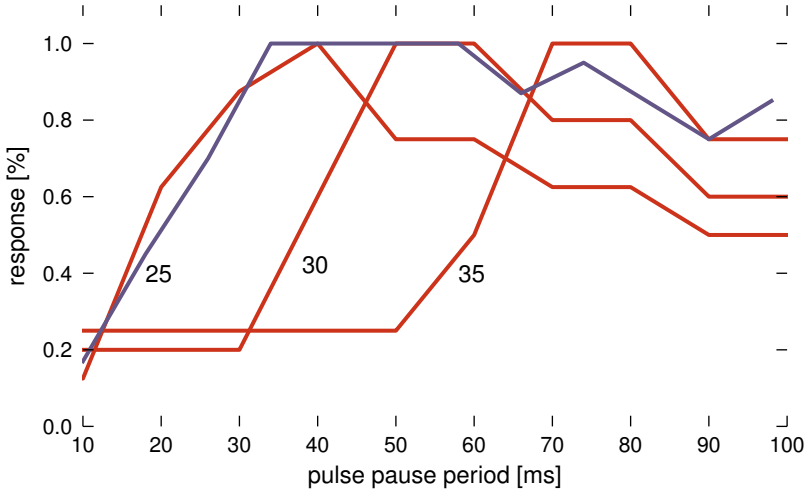


**Figure 17:** Response curves of low-pass filters using synaptic depression. The numbers in the plot indicate the values for $\tau_d$ in ms. All other parameters are as in figure 14. The purple line represents the low-pass filter extracted from Schildberger [Schildberger, 1984] (cf. figure 3).

high-pass pulse counter shown in figure 15. In figure 18 it can be seen, that a certain amount of synaptic depression is still necessary for the pulse counter to function as a high-pass filter. If $\tau_d$ is sufficiently small, the unit starts to produce several spikes per pulse. Since the duty-cycle in the Schildberger-set-up is constant, this eventually leads to a flat filter response curve. The superimposed Schildberger line again shows, that a filters in the relevant frequency range can be produced using this approach.

Figure 19 finally shows the filters found by Schildberger with the superimposed closest matching short-term plasticity filters. The low and high-pass units can reasonably approximate the physiological data. The band-pass like filter shown in orange in the figure can not be reproduced by simple depression or facilitation of synapses. The filter is however attributed to a BNC2 cell, which only receives input from BNC1 units [Schildberger, 1984]. The assumption can therefore be made that a band-pass like behaviour could simply be the result of a summation of the outputs of low-pass and high-pass filters. This is indicated in the figure by the dashed orange line, which represents the normalised sum of the responses of the other two filters.

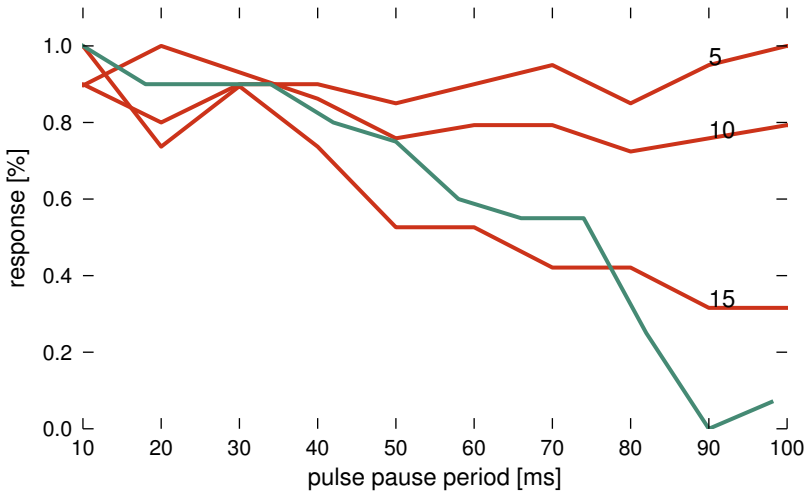


**Figure 18:** Response curves of high-pass filters using synaptic depression. The numbers in the plot indicate the values for $\tau_d$ in ms. All other parameters are as in figure 15. The turquoise line represents the high-pass filter extracted from Schildberger [Schildberger, 1984] (cf. figure 3).

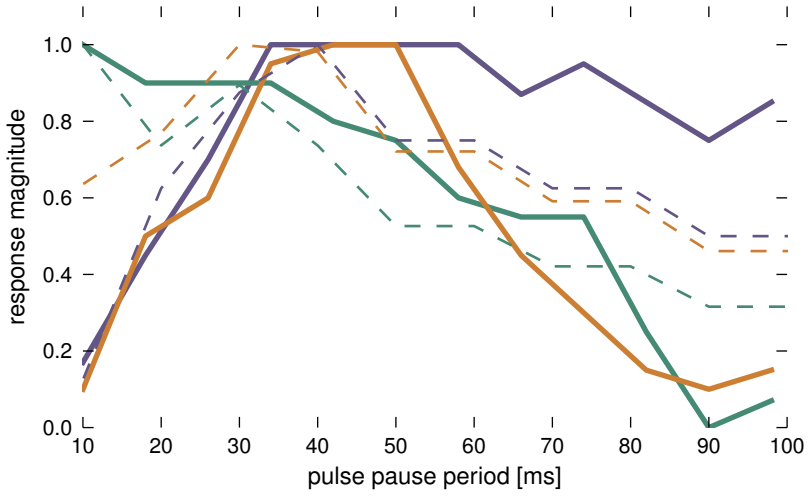


**Figure 19:** Schildberger's filter curves extracted from [Schildberger, 1984] are shown as solid lines. The dashed lines represent the closest matching filter obtained with short-term plasticity. The dashed orange line is the normalised sum of the other two dashed lines.

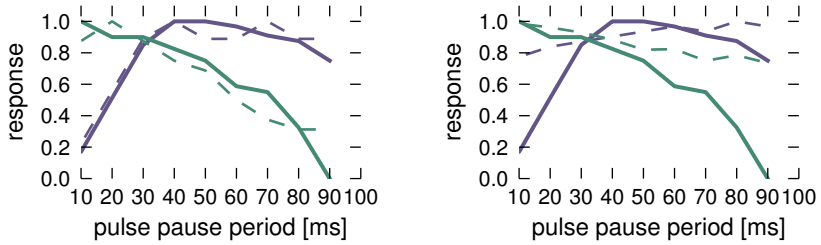


(a) with synaptic plasticity (b) without synaptic plasticity

**Figure 20:** The closest matching results of the two parameter searches superimposed as dashed lines on the Schildberger filters.

# 5 Discussion

The present study proposes that short-term synaptic plasticity may be the source of the filter-properties of the BNC neurons in the cricket *Gryllus bimaculatus*. The fact that synaptic depression has been found to be involved in drosophila olfactory processing [Kazama & Wilson, 2008] makes it at least plausible, that such mechanisms could also be found in the cricket brain. It has been shown that filters can be constructed in a simple way, which are able to reproduce the filters reported by Schildberger [Schildberger, 1984]. The membrane potentials of the filters constructed (see figures 13 through 15) even show some resemblance to the intracellular recordings of some BNC cells in [Schildberger, 1984].

The paradigm used by Schildberger has some important shortcomings. By keeping the duty cycle of the patterns constant, it was made impossible to distinguish between pulse-filters and pause-filters [Hennig, 2003]. This means that filters which perform well in this set-up may perform considerably worse when pulse and pause duration are varied independently. Schildberger has indicated the behaviourally measured phonotactically effective region in his filter plot [Schildberger, 1984]. It corresponds more or less to the band-pass filter curve shown in figure 3 as an orange line. As already indicated in section 4.3, this trace is attributed to a BNC2 cell, which may simply combine the outputs of of several BNC1 cells with varying filter properties. It can be seen in figure 19 that this can easily be achieved for Schildberger's constant duty cycle case. For the 2D pulse pause field, this would mean that such a BNC2 unit should produce a response that has a shape similar to the behavioural data shown in figure 2. To investigate the plausibility of such a set-up using the filters proposed here, a simulation was run over the entire pulse-pause field shown in

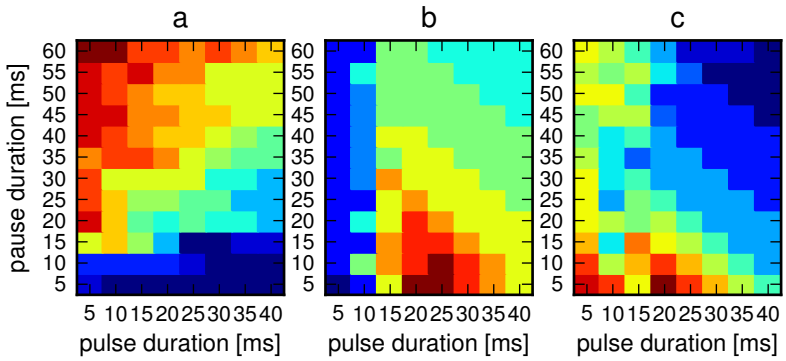


**Figure 21:** Response of the three best STP filters to the pulse-pause field varied over the same range as in figure 2. **a**: low-pass facilitation **b**: low-pass depression **b**: high-pass depression

figure 2 for all three filter types. The results of this simulation are shown in figure 21. Although some diagonal structures hinting at the shape observed in figure 2 can be seen at least in plots **b** and **c**, it is hard to see, how a linear combination of these patterns could reproduce the behaviourally efficient shape.

The filters presented in the present study made only use of either isolated synaptic depression or isolated facilitation. A parameter search allowing combinations of the two has shown however, that more complex filters can be achieved using the model (see figure 20(a)). These filters however are not as straightforward to analyse and have not been investigated in more detail. To rule out the possibility, that such filters could also be constructed without the use of synaptic plasticity, a parameter search was performed, where all parameters of the neuron model described in section 3.1 were varied over a wide range. No satisfactory filtering properties could be obtained in this way (see figure 20(b)).

Further work on the subject should involve a thorough analysis of pulse-pause filter properties of STP-synapses, possibly involving an analytical description. Also, the way the filter-properties were analysed here were adapted to the results of Schildberger to allow a comparison. This scenario is however not biologically realistic. Crickets are normally exposed to chirp patterns containing 4 or 5 pulses interrupted by longer chirp pauses. It has to be investigated in a next step, whether the filters described here can also perform in such a scenario. It is likely that the high-pass filter, which basically depends on the number of pulses in the counting window will not yield any useful information in such a case.

The concept of fitting a BNC2 - like summation unit to the model will also re-

quire further work. It is not clear how the integration over realistic calling songs can be achieved. During the parameter-study involving no STP, it became evident, that long time-constants of adaptation may lead to a filtering effect with respect to the longer time-scale chirp structure of the cricket songs. It should therefore be investigated whether the implementation of separate pulse and chirp filters as proposed by Hennig [Hennig, 2009] could be implemented by combining the proposed filters in parallel with a simple adapting unit that filters chirp-pauses.

It is hoped that physiologists will examine the relevant cells in the cricket brain further, so that a better understanding of the filtering mechanisms can be gained. Data as shown in figure 21 for real BNC neurons would enable a solid judgement as to whether the mechanism proposed here bears any resemblance to the biological ones.

# 6 Conclusion

In this study, a biologically plausible mechanism for the discrimination cricket calling songs in the brain of *Gryllus bimaculatus* has been proposed. Ignoring other aspects of phonotactic processing, like directional cues and song intensity, a model of the cricket's auditory tract has been produced. For this purpose, extracellular recordings of the ascending neuron 1 (AN1) from 13 animals have been analysed. The firing-rate levels and adaptive properties of the cells have been characterised, and a *standard AN1* has been fitted to the median values found in the data using an adaptive leaky integrate and fire model. The model-rates compare well to the physiological data, when fed with pattern envelopes in form of direct current injections. The model is believed to capture the aspects of the AN1 response which are relevant to the recognition of attractive calling songs.

It has been argued, that the existence of short-term synaptic plasticity in the cricket brain is biologically plausible, and that such mechanisms are able to implement useful filter properties. Using a phenomenological model that produces short term depression as well as facilitation, it was demonstrated on three simple examples that low-pass and high-pass filters can be constructed using only facilitation or depression, which perform well in the paradigm described by Schildberger [Schildberger, 1984]. These filters are well understood, and their frequency response can be controlled by varying the time constants of the plasticity model. Such tuning yielded good agreement with the filters reported by Schildberger.

Further, it was discussed that the mechanisms presented here are unlikely

to capture the discrimination of patterns over the full range of possible pulse and pause durations. A parameter search over a large range has however indicated, that more complex filters can be generated using combinations of depression and facilitations. Since these effects have not yet been fully understood, no description of these filters have been given here, but the task has been left open for further study.

It has been indicated, that further studies should also investigate the behaviour of those filters outside of the narrow Schildberger-paradigm. This should also incorporate a consideration of more complex patterns, involving also the full chirp-structure of the cricket's calling song. The addition of a BNC2-like cell to the model, which sums up the filter outputs of the proposed BNC1 units, possibly combined with a chirp filter based on spike frequency adaptation with long effective time constants, may lead to a complete model of the cricket's pattern recognition apparatus.

Finally, more physiological evidence about the BNC-units will allow a better assessment of the model proposed here.

## References


[Benda & Hennig, 2008] Benda, J. & Hennig, R. M. (2008). Spike-frequency adaptation generates intensity invariance in a primary auditory interneuron. *Journal of computational neuroscience*, 24(2), 113–36.

[Boyan & Williams, 1982] Boyan, G. & Williams, J. L. D. (1982). AUDITORY NEURONES IN THE BRAIN OF THE CRICKET GRYLLUS BIMACULATUS (DE GEER): ASCENDING INTERNEURONES. *J. Insect Physiology*, 28(6), 493–501.

[Faulkes & Pollack, 2000] Faulkes, Z. & Pollack, G. S. (2000). Effects of inhibitory timing on contrast enhancement in auditory circuits in crickets (Teleogryllus oceanicus). *Journal of neurophysiology*, 84(3), 1247–55.

[Fox et al., 1988] Fox, R. F., Gatland, I. R., Roy, R., & Vemuri, G. (1988). Fast exponentially correlated colored noise. *Physical Reviews A*, 38(11).

[Hedwig, 2006] Hedwig, B. (2006). Pulses, patterns and paths: neurobiology of acoustic behaviour in crickets. *Journal of comparative physiology. A, Neuroethology, sensory, neural, and behavioral physiology*, 192(7), 677–89.

[Hedwig & Poulet, 2005] Hedwig, B. & Poulet, J. F. a. (2005). Mechanisms underlying phonotactic steering in the cricket Gryllus bimaculatus revealed

with a fast trackball system. *The Journal of experimental biology*, 208(Pt 5), 915–27.

[Hennig, 2003] Hennig, R. M. (2003). Acoustic feature extraction by cross-correlation in crickets? *Journal of comparative physiology. A, Neuroethology, sensory, neural, and behavioral physiology*, 189(8), 589–98.

[Hennig, 2009] Hennig, R. M. (2009). Walking in Fourier's space: algorithms for the computation of periodicities in song patterns by the cricket Gryllus bimaculatus. *Journal of comparative physiology. A, Neuroethology, sensory, neural, and behavioral physiology*, 195(10), 971–87.

[Hildebrandt, esis] Hildebrandt, K. J. (2004, Diploma Thesis). Selektivitaet oder Abbildungstreue? - Untersuchungen zur neuronalen Kodierung zeitlicher Muster in der Hoerbahn von Grillen.

[Hoy, 1974] Hoy, R. R. (1974). Genetic Control of Acoustic Behavior in Crickets. *Integrative and Comparative Biology*, 14(3), 1067–1080.

[Kazama & Wilson, 2008] Kazama, H. & Wilson, R. I. (2008). Homeostatic matching and nonlinear amplification at identified central synapses. *Neuron*, 58(3), 401–13.

[Muller et al., 2007] Muller, E., Buesing, L., Schemmel, J., & Meier, K. (2007). Spike-frequency adapting neural ensembles: beyond mean adaptation and renewal theories. *Neural computation*, 19(11), 2958–3010.

[Nabatiyan et al., 2003] Nabatiyan, a., Poulet, J. F. a., de Polavieja, G. G., & Hedwig, B. (2003). Temporal pattern recognition based on instantaneous spike rate coding in a simple auditory system. *Journal of neurophysiology*, 90(4), 2484–93.

[Nawrot et al., 2010] Nawrot, M., Krofzcik, S., Farkhooi, F., & Menzel, R. (2010). Fast dynamics of odor rate coding in the insect antennal lobe. *arXiv:1101.0271v1*.

[Pollack, 2000] Pollack, G. (2000). Who, what, where? Recognition and localization of acoustic signals by insects. *Current opinion in neurobiology*, 10(6), 763–7.

[Schildberger, 1984] Schildberger, K. (1984). Temporal selectivity of identified auditory neurons in the cricket brain. *Journal of Comparative Physiology A*, 155(2), 171–185.

[Schildberger, 1988] Schildberger, K. (1988). Behavioral and neuronal mechanisms of cricket phonotaxis. *Motor Control*, 44, 408–415.

[Tripp & Eliasmith, 2010] Tripp, B. P. & Eliasmith, C. (2010). Population models of temporal differentiation. *Neural computation*, 22(3), 621–59.

[Tsodyks et al., 1998] Tsodyks, M., Pawelzik, K., & Markram, H. (1998). Neural networks with dynamic synapses. *Neural computation*, 10(4), 821–35.

[Webb & Scutt, 1997] Webb, B. & Scutt, T. (1997). A spiking neural model of cricket phonotaxis. In *Fourth European Conference on Artificial Life*.

[Wittmann et al., 2010] Wittmann, J. P., Kolss, M., & Reinhold, K. (2010). A neural network-based analysis of acoustic courtship signals and female responses in Chorthippus biguttulus grasshoppers. *Journal of computational neuroscience*.

[Wohlers & Huber, 1978] Wohlers, D. W. & Huber, F. (1978). Intracellular recording and staining of cricket auditory interneurons (Gryllus campestris L.,Gryllus bimaculatus DeGeer). *Journal of Comparative Physiology ? A*, 127(1), 11–28.